Time multiplexing super resolution using a 2D Barker-based array

Asaf Ilovitsh[1], Tali Ilovitsh[1], Eyal Preter[1], Nadav Levanon[2], and Zeev Zalevsky[1]

[1]Faculty of Engineering, Bar-Ilan University, Ramat-Gan 5290002, Israel

[2]School of Electrical Engineering, Faculty of Engineering, Tel-Aviv University, Tel-Aviv 6997801, Israel

ABSTRACT

We propose the use of a two dimensional Barker-based array in order to improve the performance of the standard time multiplexing super resolution system. The Barker-based array is a 2D generalization of the standard 1D Barker code. It enables achieving a two dimensional super resolution image using only one dimensional scan, by exploiting its unique auto correlation property. A sequence of low resolution images are captured at different lateral positions of the array, and are decoded properly using the same array. In addition, we present the use of a mismatched array for the decoding process. The cross correlation between the Barker-based array and the mismatched array has a perfect peak to sidelobes ratio, making it ideal for the super resolution process. Also, we propose the projection of this array onto the object using a phase-only spatial light modulator. Projecting the array eliminates the need for printing it, mechanically shifting it, and having a direct contact with the object, which is not feasible in many imaging applications. The proposed method is presented analytically, demonstrated via numerical simulation, and validated by laboratory experiments.

Key words: Super resolution; Image processing; Phase-only filters; Spatial light modulators.

1. INTRODUCTION

A perfect imaging lens with a finite aperture is diffraction limited. This dictates a restriction on the minimal distance at which two point sources can be resolved using this lens. The minimal distance was defined by Abbe to be proportional to the optical wavelength, and to the F number of the imaging system [1]. One of the most common methods of super resolution (SR) which overcomes the diffraction limitation is time multiplexing super resolution (TMSR), originally suggested by Francon [2]. These techniques improve the spatial resolution at the expense of the time domain using some *a priori* knowledge on the inspected object. The main concept was proposed by Lukosz [3], and includes the use of two moving gratings that are shifted between time frames during the imaging sequence. The first grating is placed near the object and encodes the spatial information, and the second grating is placed near the image and decodes the spatial information. The second grating may be added digitally via computer means [4].

For a 1D SR, the gratings shift is relatively simple. However, in order to achieve 2D SR, the gratings need to be shifted in both directions. Another approach is using a random noise as the encoding and decoding masks [5]. This method relies on the auto-correlation (AC) of the random noise mask. Since the noise is random in all direction, a 1D shift can achieve 2D SR. However, the variance of the sidelobes of the AC is in the order of the square root of the number of images. Thus, reducing the variance of the sidelobes requires a great number of images, usually hundreds. Another method is regarding the SR process as an inverse problem [6]. This method has an inherent difficulty, which is to avoid amplifying the noise during the inverse process (this is common for all inverse problems). In addition, the system matrix itself is ill conditioned, presenting the challenge of inverting the matrix in a numerically stable fashion [7].

1.1. Barker-based array

We propose using a binary transmission Barker-based array as the encoding and decoding mask in the conventional TMSR method [8]. The proposed array is a 2D generalization of the 1D Barker code [9], which is widely used in radar signals [10]. The proposed method has several advantages over the previous ones; a 1D scanning generates 2D SR,

Optical Methods in Developmental Biology IV, edited by Andrew M. Rollins, Scott E. Fraser, Michael A. Choma,
Proc. of SPIE Vol. 9716, 97160I · © 2016 SPIE · CCC code: 1605-7422/16/$18 · doi: 10.1117/12.2206198

regardless of the scanning direction. The process requires significantly less images than the random noise method. The method does not require invert process, and thus noises effects will not be amplified during the SR process.

A Barker code is an N length sequence of digits, where each bit has a value of -1 or 1. The Barker code has an ideal a-periodic AC property, such that the peak magnitude of the AC equals N, and the sidelobes magnitudes are 0 or 1. The Barker codes also have a two-valued cyclic (periodic) AC. This means that the sidelobes AC value of a cyclic Barker code has a constant value. In optical amplitude masks, the value -1 is not valid, since there cannot be a negative number in an amplitude mask. Thus, each -1 in the Barker code is replaced by 0. This modified Barker sequence maintains its two-valued cyclic AC property. A 2D unipolar Barker array will be optimal for TMSR. Unfortunately, this kind of array does not exist for more than 2x2 array [11,12]. Instead, a generalization of the Barker code into a 2D array was performed as follows; the first row in the array is a standard 1D Barker code, and each row in the array is shifted with respect to the previous row.

The longest reported Barker code is 13bit long [13]. Using its unipolar representation [1111100110101], a 13x13 array was established. The process is as follows, each row in the array is shifted 5 pixels to the right in respect to the previous row. This 2D array is presented in Fig. 1(a). One may notice that by using the 5 pixels shift between rows, each column in the array is a cyclic shift of a 13bit Ipatov code [1110010111110] [10] which, while not Barker, also exhibits a two-valued cyclic AC. The cyclic AC of the 13x13 example is presented in Fig. 1(b). The cyclic AC has N peaks equal to 1, with a distance between each two peaks of $\sqrt{13}$. The sidelobes between the peaks has a constant value of 2/3.

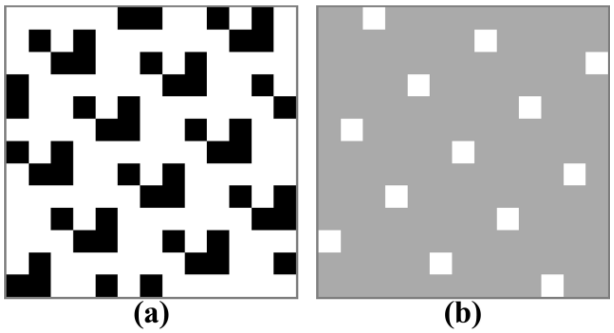

Fig. 1. (a) A 13x13 Barker-based array, where each row is a 5 pixels shift of the previous row. (b) The cyclic AC of the 13x13 Barker-based array. Pixels values; white: 1, gray: 2/3, black: 0.

Following the conventional TMSR 4f system (presented in Fig. 2), the blurred output intensity, just before the second mask, is given by:

$$I_{img}(x,y,t)=\int_{-\infty}^{\infty}\int_{-\infty}^{\infty} I_{obj}(x',y')M_1(x'-vt,y')\,p(x-x',y-y')dx'dy' \tag{1}$$

where I_{obj} is the object intensity, M_1 is the encoding mask, v is its velocity, and p is the point spread function (PSF).

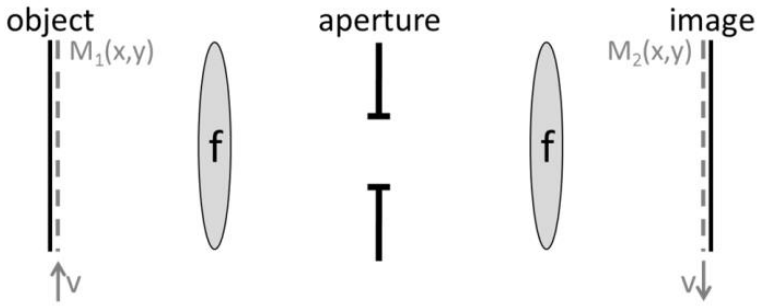

Fig. 2. A conventional TMSR 4f system.

The decoding process involves multiplying each image with the appropriate decoding mask M_2, and integrating over time:

$$R(x,y)=\int_{-\infty}^{\infty} I_{img}(x,y,t)M_2(x-vt,y)dt \tag{2}$$

Since only the masks are time depended, changing the integral order is allowed. Assuming M_1 and M_2 are the same Barker-based array, denoted by M, the time integral becomes:

$$\int_{-\infty}^{\infty} M(x-vt,y)M(x'-vt,y')dt=\sum\delta(x-x',y-y')+c \tag{3}$$

The result is a set of Dirac deltas plus a constant (as presented in the 13bit example in Fig. 1(b)). Introducing the time integral into Eq. (3) yields:

$$R(x,y)=\int_{-\infty}^{\infty}\int_{-\infty}^{\infty} I_{obj}(x',y')\,p(x-x',y-y')\left[\sum\delta(x-x',y-y')+c\right]dx'dy' \tag{4}$$

Assuming the PSF is smaller than the distance between two peaks, the integral becomes:

$$R(x,y)=p(0,0)I_{obj}(x,y)+c\cdot LRI \tag{5}$$

where LRI is the LR image.

In order to achieve the HR image, the LR image (which is known) needs to be subtracted from the reconstruction. As mentioned before, the method will work as long as the PSF is smaller than the distance between peaks, which in our examples is $\sqrt{13}$ or 3.6 pixels in the image plane.

1.2. Mismatched array

For the decoding mask, a mismatched filter can also be used [14]. Since the process is in 2D, the mismatched filter is also an array. The mismatched array is based on the same Barker-based array, with the following change: each pixel of 0 in the array is transformed into -2. For example, the first row in the mismatched array is [11111-2-211-21-21]. Since the decoding mask is added digitally, negative values are allowed. The cyclic cross correlation (CC) of the Barker-based array with the mismatched array has a perfect peak to sidelobes ratio. Namely, it has N peaks equal to 1, and sidelobes between the peaks that equal 0. The distance between each two peaks is $\sqrt{13}$. The 2D Barker-based array is presented in Fig. 1(a), and the CC with the mismatched array is presented in Fig. 1(b).

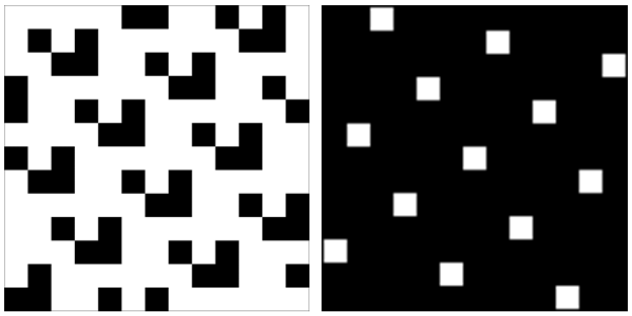

Fig. 3. (a) A 13x13 Barker-based array, where each row is a 5 pixels shift of the previous row. (b) The cyclic CC of the 13x13 Barker-based array with the mismatched array. Pixels values; white: 1, black: 0.

In this case, the constant c in Eq. (3) is zero, and therefore, Eq. (5) is simplified to:

$$R(x,y) = p(0,0)I_{obj}(x,y) \tag{6}$$

Which means that in the case of the mismatched array the reconstruction is exactly the high resolution (HR) image, up to a constant.

1.3. Array projection

In standard TMSR the Barker-based array needs to be printed, placed on top of the object, and mechanically shifted. This approach, though valid, suffers from a lot of engineering problems. Manufacturing issues related to the array, and mechanical shift that requires moving parts in the setup. However, the main problem is that it requires direct contact with the inspected object, which is not possible in many imaging scenarios.

Instead, we propose projecting the Barker-based array onto the inspected object using a phase only spatial light modulator (SLM). The projection of the array solves all the above mentioned problems, as all the mask manufacturing, mechanical shifting, and interaction with the object are done digitally.

The design of the phase image, that is uploaded to the SLM, involves an iterative process which relies on the revised Gerchberg-Saxton (GS) algorithm [15,16]. The Barker-based array needs to be created on an object that is placed at a certain distance from the SLM. Therefore, the design is for a SLM phase that after certain free space propagation (FSP) will transform into the desired Barker-based array. The GS process is performed by the following method (as schematically illustrated in Fig. 6).

The amplitude A_1 is defined to be the Barker-based array, and a zero phase φ_1 is imposed in order to define the output plane E_1. This field then undergoes FSP a distance of –dz to define the input plane E_0. Since the SLM is phase only, the amplitude of E_0 is imposed to be a constant value (of ones), while the phase φ_0 is being kept. The field E_0 undergoes FSP a distance of +dz to the output plane E_1. This process is then repeated numerous iterations. In every iteration the amplitude of E_1, obtained by the FSP, is compared to the Barker amplitude. When the correlation coefficient between the two is higher than a predetermined value, the phase retrieval of the input plane is achieved. Since the GS process is performed independently from the imaging process, the time required for generating the phase masks is not significant (in our case it was a few hours).

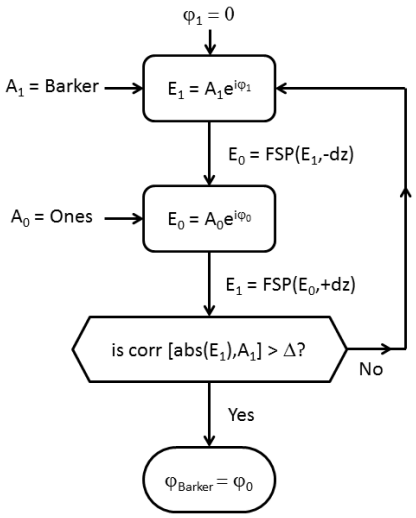

Fig. 4. Iteration flowchart of the GS process.

The results of the phase design using the revised GS process for dz=0.55m are presented in Fig. 5. This distance was chosen so that the SLM duplications in the later on experiment will not overlap. Fig. 5(a) is the desired Barker-based array, Fig. 5(b) is the phase only GS result that is uploaded to the SLM, and Fig. 5(c) is the obtained amplitude results

after FSP of the phase mask for the distance of dz. Fig. 5(d) presents the correlation coefficient between the desired Barker-based amplitude image (Fig. 5(a)) and the FSP result (Fig. 5(c)), in a semi-log scale. The correlation converges to 0.96.

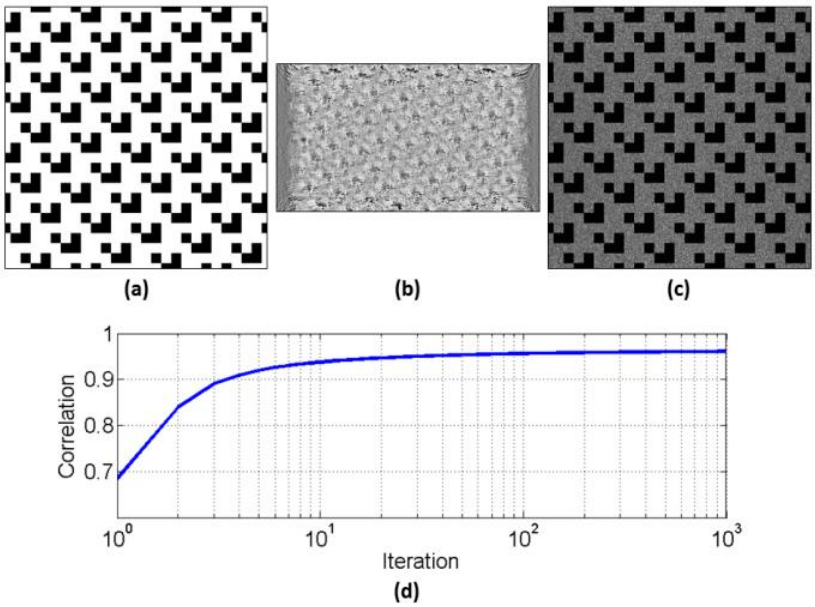

Fig. 5. Phase design using the revised GS process. (a) Desired Barker-based array. (b) The phase result that is uploaded to the SLM. (c) The amplitude results after FSP of dz=0.55m. (d). The correlation coefficient between (a) and (c) during the GS process.

2. NUMERICAL SIMULATION

In the numerical simulation the proposed 13x13 array was tested. The Barkar-based masks were cyclic, in order to cover the entire object. The masks speed was 1 pixel per frame. 13 LR images which simulated the mask movement were generated. The LR images had resolution which is 3 times smaller than the HR images. The suggested process was tested on a 1951 USAF target. The SR results are presented in Fig. 6. Fig. 6(a) is the HR image, Fig. 6(b) is the LR image, Fig. 6(c) is the reconstructed image using 13 LR images of a moving random mask, and Fig. 6(d) is the SR image using the Barker-based mask. It is clearly seen that the proposed method yields better results than the random mask method.

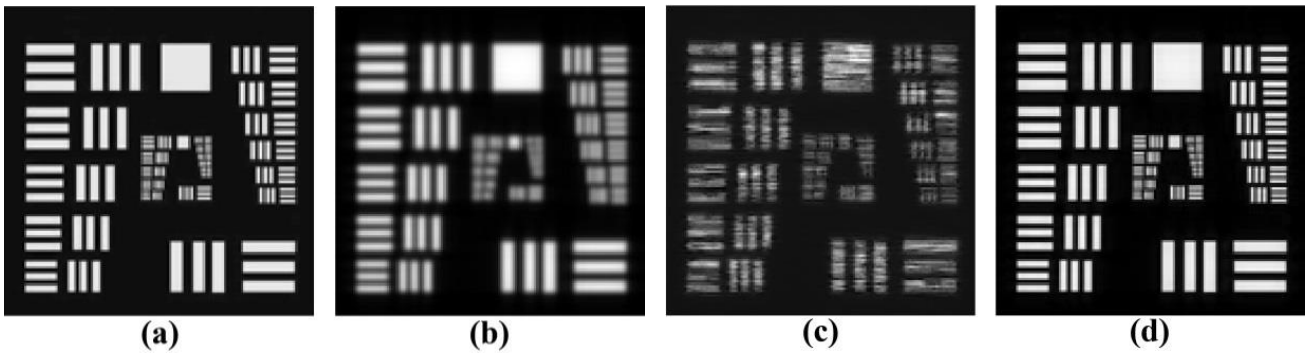

Fig. 6. SR simulation results of a USAF target using the proposed 13x13 Barker-based array. (a) HR image. (b) LR image. (c) Reconstructed image using a moving random mask. (d) SR using the Barker-based mask.

3. EXPERIMENTAL RESULTS

In order to experimentally test the proposed method, two experimental setups were built. The first is aimed to test a printed Barker-based array, and the second is for projecting the array via SLM, and using the mismatched array for decoding.

3.1. Printed array

In this experiment, a simple imaging system was built in the laboratory. The object was a USAF target. The mask was a 13x13 cyclic Barker-based array, with a 1mm feature size. The mask was placed on top of the object, and shifted laterally in 1mm increments using a linear translation stage. 13 LR images were captured using a standard USB camera (Thorlabs DCC1545M), and an 8mm lens (Navitar NMV-8) located 500mm above the object. The mask feature size was chosen in order to fulfill the spatial sampling condition [17], making sure that it is sampled at least twice by the camera pixels. This has two implications; first, the resolution improvement is limited to the mask feature size (which is about 3x3 pixels in the object plane), and second, the LR PSF needs to be smaller than the distance between the AC peaks, which in this case is $3\cdot\sqrt{13}$ or 10.8 pixels in the image plane. The LR images in the experiment had resolution about 9 times smaller than HR reference images. The setup illustration is presented in Fig. 7.

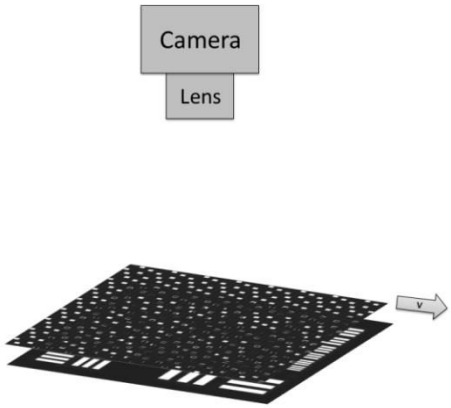

Fig. 7. Experimental setup illustration. A camera looking down on a 1951 USAF target, covered by a moving cyclic Barker-based array.

The SR results, obtained using the proposed technique, are presented in Fig. 8. Fig. 8(a) is the HR reference image. Fig. 8(b) is the LR image, and Fig. 8(c) is the SR image. The resolution improvement is clearly visible, not only in the marked bars, which mark the last separable frequency, but also in the numbers in the target. One may notice that the SR image is pixelate, with feature size of about 3x3 pixels, due to the feature size of the encoding mask.

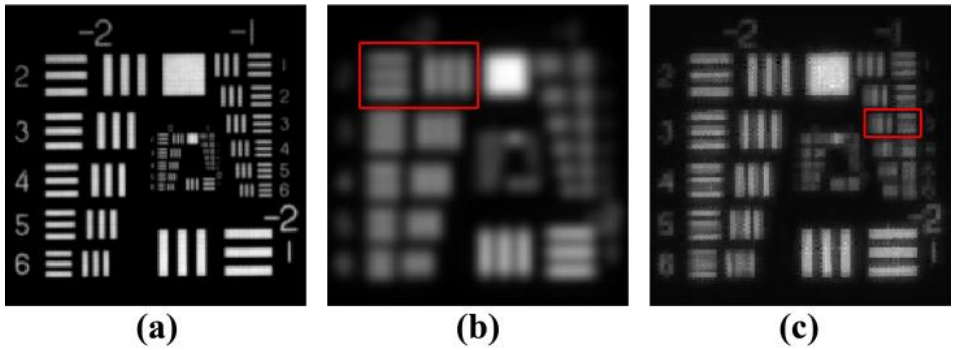

Fig. 8. SR experimental results. (a) HR object. (b) LR image. (c) SR image using the proposed method. The squares represent the last separable frequency in the LR and SR images.

3.2. Projected array

The projection method was tested using the experimental setup which is presented in

Fig. 9. The setup is divided into two main parts, projection and imaging. The projection part consists of a green laser beam at a wavelength of 532 nm (Photop DPGL-2100F), a ×3 beam expender (Newport T81-3X), and a ×10 beam expender (Thorlabs BE10M-A). The total ×30 expansion of the laser beam is required in order to achieve an almost uniform illumination of the SLM. The SLM is a phase-only reflective liquid-crystal-on-silicon micro display with 1920×1080 pixels resolution and pixel's pitch of 8μm (Holoeye SLM device HEO 1080P). The object was a USAF target located 550mm from the SLM. The imaging part consists of a 50mm imaging lens (Navitar MVL50M23), located 500mm from the object, and a USB camera (Thorlabs DCC1545M).

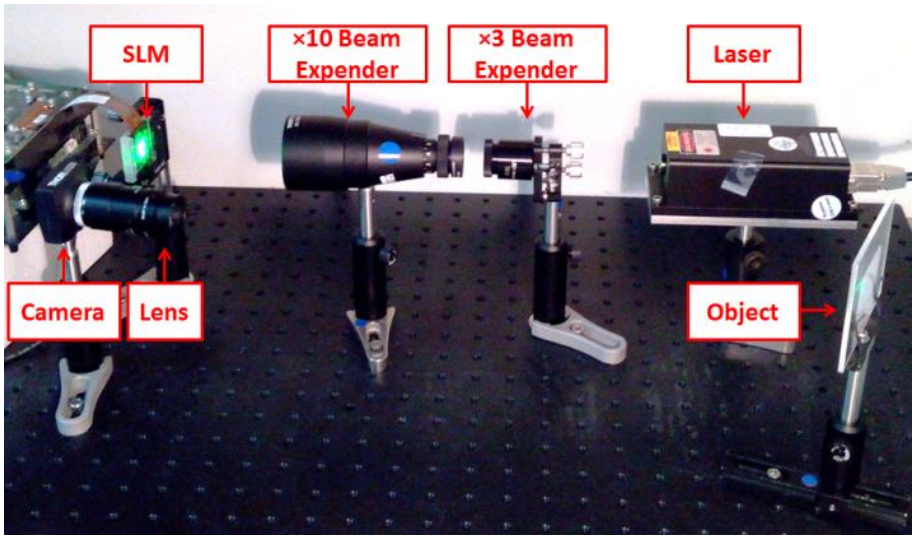

Fig. 9. The experimental setup. A green laser, expended ×3, and then ×10, illuminating the SLM and reflected onto the object. The object is then imaged by a lens and a camera.

13 different phase masks were displayed using the SLM. Each phase mask generates a shifted Barker-based array at the object plane. 13 low resolution (LR) images were captured, each one corresponding to a specific position of the array. The LR images in the experiment had resolution about 20 times smaller than HR reference images. The Barker-based array feature size at the object plane was ~0.4mm, which translates to ~8.5 pixels in the camera.

The SR results, obtained using the proposed technique, are presented in Fig. 10(a) is the HR reference image, Fig. 10(b) is the LR image, and Fig. 10(c) is the SR image, achieved using the projected Barker-based array, and the mismatched filter. The resolution improvement is clearly visible.

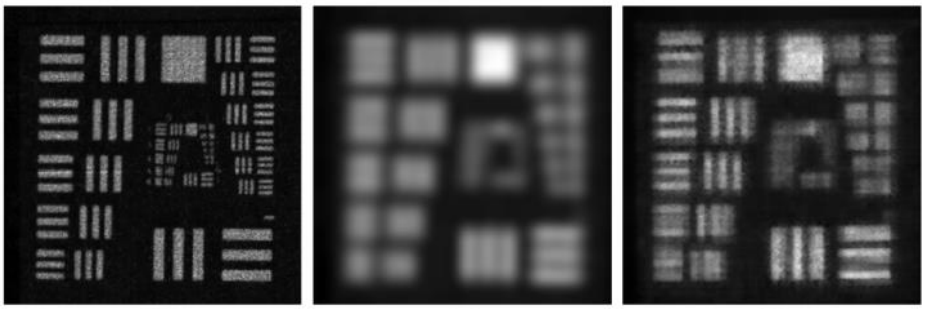

Fig. 10. SR experimental results. (a) HR object. (b) LR image. (c) SR image using the proposed method.

CONCLUSIONS

A 2D Barker-based array, which is a generalization of the well-known 1D Barker code, was presented. Due to the unique AC properties of the proposed array, only a small number of images are required in order to achieve TMSR. The use of a mismatched array, with perfect CC properties allows SR imaging with even simpler computations. Projecting the array, instead of placing it directly on the object, offers a much more flexible imaging system, that can be suitable to more complex scenarios where accessing the object is not feasible. The phase calculation process using the revised GS algorithm, and laboratory experiments demonstrating the proposed concept were presented.

REFERENCES

[1] Otto, R., and Fritz, L., [Die lehre von der bildentstehung im mikroskop von Ernst Abbe], Vieweg Braunschweig (1910).

[2] Françon, M., "Amélioration de résolution d'optique," Nouvo Climento Suppl. 9, 283–290 (1952).

[3] Lukosz, W., "Optical systems with resolving powers exceeding the classical limit," Journal of the Optical Society of America 56(11), 1463–1471 (1966).

[4] Shemer, A., Mendlovic, D., Zalevsky, Z., Garcia, J., and Martinez, P.G., "Superresolving optical system with time multiplexing and computer decoding," Applied optics 38(35), 7245–7251 (1999).

[5] García, J., Zalevsky, Z., and Fixler, D., "Synthetic aperture superresolution by speckle pattern projection.," Optics Express 13(16), 6073–6078 (2005).

[6] Farsiu, S., Robinson, D., Elad, M., and Milanfar, P., "Advances and challenges in super-resolution," International Journal of Imaging Systems and Technology 14(2), 47–57 (2004).

[7] Golub, G.H., and Van Loan, C.F., [Matrix Computations] , in Matrix Comput., The Johns Hopkins University Press (1996).

[8] Ilovitsh, A., Preter, E., Levanon, N., and Zalevsky, Z., "Time multiplexing super resolution using a Barker-based array," Optics letters 40(2), 163–165 (2015).

[9] Barker, R.H., "Group Synchronizing of Binary Digital Sequences," Communication Theory, 273–287 (1953).

[10] Levanon, N., and Mozeson, E., [Radar signals], John Wiley & Sons (2004).

[11] Alquaddoomi, S., and Scholtz, R.A., "On the nonexistence of Barker arrays and related matters," IEEE Transactions on Information Theory 35(5), 1048–1057 (1989).

[12] Davis, J. a., Jedwab, J., and Smith, K.W., "Proof of the Barker array conjecture," Proceedings of the American Mathematical Society 135(07), 2011–2019 (2007).

[13] Turyn, R., and Storer, J., "On binary sequences," Proceedings of the American Mathematical Society 12(3), 394–399 (1961).

[14] Ilovitsh, A., Ilovitsh, T., Preter, E., Levanon, N., and Zalevsky, Z., "Super-resolution using Barker-based array projected via spatial light modulator," Optics Letters 40(8), 1802–1805 (2015).

[15] Gerchberg, W.R., and Saxton, W.O., "A practical algorithm for the determination of phase from image and diffraction plane pictures," Optik 35, 237–246 (1972).

[16] Gur, E., and Zalevsky, Z., "Image deblurring through static or time-varying random perturbation medium," Journal of Electronic Imaging 18, 033016 (2009).

[17] Goodman, J.W., [Introduction to fourier optics] , Roberts & Company (2005).